ELSEVIER

Solar Energy Materials and Solar Cells 32 (1994) 463–476

Solar Energy Materials and Solar Cells

Three-particle correlations in the optical properties of granular composites

Rubén G. Barrera [a,*], Carlos I. Mendoza [a,b]

[a] *Instituto de Física, Universidad Nacional Autónoma de México, Apdo. Postal 20-364, 01000 México, Distrito Federal, México*

[b] *Facultad de Ciencias, UNAM, 04510 México, Distrito Federal, México*

(Received 29 November 1993)

Abstract

The effective dielectric response of a system of spherical inclusions embedded in an otherwise homogeneous matrix has been calculated using, in the Maxwell Garnett formula, a renormalized polarizability instead of the bare one (Phys. Rev. B 38, 5371 (1988)). This renormalized polarizability was given as a functional of the two- and three-particle distribution functions and results were presented for a very crude approximation of the three-particle distribution function. Here we extend these results and analyze the effects of the three-particle correlations by using the best available form of this functional. We compare our results with other theoretical approaches and recent numerical simulations.

1. Introduction

The interest in the electrical and optical properties of granular media dates back to the beginning of electrodynamics. The problem of calculating the effective conductivity of a system of insulating spheres embedded in a conducting matrix is already solved in the works of J.C. Maxwell [1], in the extreme-dilute limit, and of Lord Rayleigh for a periodic array [2]. Later on, at the beginning of this century, J.C. Maxwell Garnett [3] studies the optical properties of a system of conducting spheres embedded in an insulating matrix. He obtains a relation for the effective dielectric function of the system in terms of the filling fraction of the spheres and the dielectric functions of each component. A very complete review of the early

* Corresponding author.

0927-0248/94/$07.00
SSDI 0927-0248(93)E0134-Y

history of this problem can be found in the beautiful article of Landauer presented at the first ETOPIM conference [4]. Recently there has been a renewed interest in this problem due to the development of new theoretical methods for the treatment of disordered systems [5], and also due to the potential use of granular composites in selectively absorbing paints for solar energy devices [6].

It is now recognized that the Maxwell Garnett (MG) solution corresponds, within a statistical approach, to a mean-field theory within the dipolar, quasistatic approximation. It can also be easily shown that it is completely equivalent to the well-known Clausius–Mossotti relation [7] in the dielectric theory of liquids. The most remarkable feature of the MG solution is that the only statistical property of the distribution of inclusions, that appears in the theory, is the filling fraction of the spheres. Now we know that this is quite fortuitous and that it happens only in the very special case of spherical inclusions in a 3D system. As soon as one considers either a system of spheres located at random in 2D [8] or non-spherical inclusions in a 3D system [9], one finds that the effective dielectric response (EDR) in the dipolar, quasistatic, mean-field approximation requires of more information about the microstructure of the system: it depends not only on the filling fraction of the spheres but also in their two-particle distribution function.

In the mean-field approximation (MFA) the fluctuations in the induced dipoles are neglected, that is, the induced dipoles at each sphere are considered all the same and equal to their mean (average) value. In this approximation the EDR shows a resonance which is red-shifted with respect to the corresponding dipolar resonance of the isolated sphere. This is also called the dipolar resonance of the system and the amount of red-shift increases as the filling fraction increases.

On the other hand, it is now generally accepted [10–12], that the main effect of the dipolar fluctuations in the EDR is to produce an additional broadening and a strong asymmetry of the dipolar resonance, at *all* filling fractions. Additional here means, *additional* to the usual broadening produced by the non-radiative energy-loss mechanisms. Since in an ordered system there are no dipolar fluctuations, these fluctuations are due to the effects of disorder, thus this additional broadening is also refereed to as *disordered induced* [11]. Furthermore, recent numerical simulations [12] show that, within the dipolar approximation, this disordered-induced broadening increases as the filling fraction of spheres increases but that it decreases back when the filling fraction gets near to its closed-packed value.

On the other hand, for high filling fractions of spheres, the dipolar approximation breaks down and higher induced multipoles start to play an important role in the EDR. It can be shown [13], that in the mean-field approximation, that is, when the induced multipolar fluctuations are neglected, there are no multipolar contributions (beyond the dipole) to the EDR when the two-particle distribution function has spherical symmetry. Only when multipolar fluctuations are taken into account or when the two-particle distribution function has no spherical symmetry, there is a net multipolar effect in the EDR. This is, for example, the case of a periodic system of spheres, which has no multipolar fluctuations, but it has a two-particle distribution function with crystalline symmetry [14]. For a homogeneous, isotropic, disordered system, numerical simulations [15] have shown that the

main effect of the multipolar fluctuations in the EDR is the appearance of multipolar resonances with its corresponding disorder-induced broadening.

In this work, we go beyond the MFA using a simple renormalization procedure for the polarizability of the spheres [11]. Our objective is to evaluate the importance of the three-particle correlations in the EDR. Since both, the multipolar corrections and the ones coming from three-particle correlations become important whenever the filling fraction gets high, here we isolate the effect of the three-particle correlations by keeping the calculation within the dipolar approximation.

2. Formalism

Lets us consider a homogeneous and isotropic ensemble of $N \gg 1$ identical spheres of radius a_0 and dielectric function ϵ_s located at random positions $\{\boldsymbol{R}_i\}$ in a host medium with dielectric function ϵ_b. The system is in the presence of a position-dependent external electric field $\boldsymbol{E}_{ex}$ oscillating with frequency ω and with wavelength much larger than a_0 and the typical separation between spheres. Under these conditions the dipole moment $\boldsymbol{p}_i$ induced at the ith sphere is given by

$$\boldsymbol{p}_i = \alpha(\omega)\left[\boldsymbol{E}_i^0 + \sum_j \overleftrightarrow{t}_{ij} \cdot \boldsymbol{p}_j\right] \tag{1}$$

where $\boldsymbol{E}_i^0$ is the electric field induced within the medium at $\boldsymbol{R}_i$ in the absence of the spheres, $\alpha(\omega) = a_0^3[\epsilon s - \epsilon_b]/[\epsilon_s + 2\epsilon_b]$ is the effective polarizability of an isolated sphere within the host medium, and

$$\overleftrightarrow{t}_{ij} = (1 - \delta_{ij})\vec{\nabla}_i\vec{\nabla}_j(1/R_{ij}) \tag{2}$$

is the dipole–dipole interaction tensor in the quasistatic limit. Here $R_{ij} \equiv |\boldsymbol{R}_i - \boldsymbol{R}_j|$ and δij is the Kronecker delta.

The macroscopic polarization field $\boldsymbol{P}_M$, defined as the average of the induced dipole moment per unit volume, is then given by

$$\mathbf{P}_M(\mathbf{R}) = n\langle \mathbf{p} \rangle = \langle \sum_i \mathbf{p}_i \delta(\mathbf{R} - \mathbf{R}_i) \rangle, \tag{3}$$

where n is the number density of spheres and $\langle \cdots \rangle$ means ensemble average. Furthermore, the polarization induced in the system by an external field is characterized by the *external* susceptibility $\overleftrightarrow{\chi}^{ex}(q, \omega)$, defined as

$$\boldsymbol{P}_M(\boldsymbol{q}, \omega) = \overleftrightarrow{\chi}^{ex}(\boldsymbol{q}, \omega) \cdot \boldsymbol{E}^{ex}(\boldsymbol{q}, \omega), \tag{4}$$

where $\boldsymbol{E}_{ex}(\boldsymbol{q}, \omega)$ and $\boldsymbol{P}_M(\boldsymbol{q}, \omega)$ are the space-time Fourier transform of the external field and the macroscopic polarization field, respectively. The term *external* susceptibility indicates that the polarization is responding to the *external* field rather than to the *average* macroscopic electric field $\boldsymbol{E}_M$, with respect to which the electric susceptibility is usually defined.

The relationship between the local, effective (or macroscopic) dielectric response $\epsilon_M(\omega)$ and the external susceptibility $\overleftrightarrow{\chi}ex(q, \omega)$ is given by [11]

$$\frac{\epsilon_b(\omega)}{\epsilon_M(\omega)} = 1 - 4\pi\epsilon_b(\omega)\chi^{ex,l}(q \to 0, \omega), \tag{5}$$

where the superscript l denotes longitudinal projection. For a non-magnetic system, the long wavelength limit of the longitudinal l and transverse t response coincides, that is, $\chi ex, l(q \to 0, \omega) = \chi ex, t(q \to 0, \omega)$. Thus, the choice of the longitudinal projection in Eq. (5) instead of the transverse one, is just a matter of convenience. Since the dipolar interaction is long-range, care must be taken when the average of such an interaction field is performed, because it might yield to the appearance of ill-defined integrals in the case of an infinite system. Here we avoid this problem by adopting the following procedure: one starts by exciting the system with a longitudinal electric field of finite wavevector $\boldsymbol{q}$, that is,

$$\boldsymbol{E}^{ex}(\boldsymbol{r}) = \hat{\boldsymbol{q}}E^{ex}e^{i(\boldsymbol{q}\cdot\boldsymbol{r}-\omega t)}, \tag{6}$$

and the linear set of equations given by Eq. (1) is solved for $\{p_i\}$. An ensemble average of $\{\boldsymbol{p}_i\}$ is then taken and the calculation of the macroscopic polarization field $\boldsymbol{P}_M$ and the external susceptibility $\overleftrightarrow{\chi}ex$ is done by using Eqs. (3) and (4), respectively. Then one takes the longitudinal projection of $\overleftrightarrow{\chi}ex$, and finally the local $\epsilon_M(\omega)$ is calculated by taking the $q \to 0$ limit of $\overleftrightarrow{\chi}ex$, l and using Eq. (5).

To follow this procedure it is convenient to introduce the following transformation

$$\mathbf{P}_i(\mathbf{q}) = \mathbf{p}_i e^{-i\mathbf{q}\cdot\mathbf{R}i}, \tag{7}$$

and

$$\overleftrightarrow{\boldsymbol{T}}_{ij}(\boldsymbol{q}) = \overleftrightarrow{\boldsymbol{t}}_{ij}e^{-i\boldsymbol{q}\cdot(\boldsymbol{R}_i-\boldsymbol{R}_j)}. \tag{8}$$

Using this transformation, Eq. (1) becomes

$$\boldsymbol{P}_i(\boldsymbol{q}) = \alpha\left[\hat{\boldsymbol{q}}E^{ex}/\epsilon_b + \sum_j \overleftrightarrow{\boldsymbol{T}}_{ij}(\boldsymbol{q})\cdot\boldsymbol{P}_j(\boldsymbol{q})\right], \tag{9}$$

where the argument ω has been omitted. The main advantage of the above transformation is that the Fourier transform of the macroscopic polarization field $\boldsymbol{P}_M$ becomes, simply

$$\mathbf{P}_M(\mathbf{q}) = N\langle\mathbf{P}_i(\mathbf{q})\rangle, \tag{10}$$

where N is the total number of inclusions.

If we now use a formal solution of Eq. (9) together with Eqs. (4) and (5) we can write

$$\frac{\epsilon_b(\omega)}{\epsilon_M(\omega)} = 1 - 4\pi\lim_{q\to 0}\left\langle\sum_j\left(\hat{\boldsymbol{q}}\cdot\overleftrightarrow{\boldsymbol{U}}(\boldsymbol{q}, \omega)\cdot\hat{\boldsymbol{q}}\right)^{-1}_{ij}\right\rangle, \tag{11}$$

where

$$\overleftrightarrow{U}_{ij}(\boldsymbol{q}, \omega) \equiv \boldsymbol{q}\delta_{ij}/\alpha(\omega) - \overleftrightarrow{T}_{ij}(\boldsymbol{q}). \tag{12}$$

Thus, one has first to invert a $N \times N$ matrix with random elements and $N \gg 1$, and then perform an ensemble average. This is obviously a non-trivial task, whose solution has lead to a wide variety of approximation schemes [16].

Here we present a simple and intuitive solution for $\epsilon_M(\omega)$ which takes account of the dipolar fluctuations in an approximate way and which reduces to the well-known MFA when these fluctuations are neglected. First we rewrite Eq. (9) as follows,

$$\boldsymbol{P}_i = \alpha\left[\boldsymbol{E}'_i + \sum_j \overleftrightarrow{\boldsymbol{T}}_{ij} . \Delta\boldsymbol{P}_j\right] \tag{13}$$

where $\Delta\boldsymbol{P}_j \equiv \boldsymbol{P}_j - \langle \boldsymbol{P} \rangle$ is the fluctuation of the jth dipolar moment,

$$\boldsymbol{E}'_i = \hat{\boldsymbol{q}}E^{ex}/\epsilon_b + \sum_j \overleftrightarrow{\boldsymbol{T}}_{ij} \cdot \langle \boldsymbol{P} \rangle, \tag{14}$$

and we have omitted the argument q. As one can see, we have written the local field at $\boldsymbol{R}_i$ as the superposition of two stochastic fields: the field $\boldsymbol{E}'_i$ generated by a collection of identical dipoles located at random positions $\{\boldsymbol{R}_j\}$ plus the field generated by the dipolar fluctuations $\Delta\boldsymbol{P}_j$ located at these same positions.

It has been shown [11], that the effects of the dipolar fluctuations in the local field can be taken into account, at least in an approximate way, by means of a single scalar parameter α^*, defined by

$$\mathbf{P}_i = \alpha^* \mathbf{E}'_i. \tag{15}$$

This parameter can be interpreted as a renormalized polarizability. Thus, we will refer to this approach as the renormalized polarizability theory (RPT). Notice that Eq. (15) looks exactly the same as the equation usually used to define the MFA [11], but with a renormalized polarizability α^* instead of the bare polarizability α. This equation can be solved immediately for $\langle \boldsymbol{P} \rangle$, and following the procedure described above yields

$$\frac{\epsilon_M - \epsilon_b}{\epsilon_M + 2\epsilon_b} = f\tilde{\alpha}^*, \tag{16}$$

which, obviously, looks exactly the same as the well-known MFA relation given by Maxwell Garnett [3], but with $\tilde{\alpha}^*$ instead of $\tilde{\alpha}$. Here $\tilde{\alpha}^* \equiv \alpha^*/a_0^3$, $\tilde{\alpha} \equiv \alpha/a_0^3$, and $f \equiv n(4\pi a_0^3/3)$ is the volume fraction of spheres.

The problem left is to find the relation between α^* and α, and this can be done by demanding consistency between Eqs. (15) and (9). One finds that $\tilde{\alpha}^*$ obeys a simple second order algebraic equation [11]

$$\frac{1}{4} f_e \tilde{\alpha}(\tilde{\alpha}^*)^2 - \tilde{\alpha}^* + \tilde{\alpha} = 0, \tag{17}$$

where

$$f_e = 4a_0^6 \lim_{q\to 0} \Delta T^2(q), \tag{18}$$

and

$$\Delta T^2(q) \equiv \left\langle \sum_{j,k} \hat{\boldsymbol{q}} \cdot \overleftrightarrow{\boldsymbol{T}}_{ij} \cdot \overleftrightarrow{\boldsymbol{T}}_{jk} \cdot \hat{\boldsymbol{q}} \right\rangle - \left\langle \sum_{j} \hat{\boldsymbol{q}} \cdot \overleftrightarrow{\boldsymbol{T}}_{ij} \cdot \hat{\boldsymbol{q}} \right\rangle^2, \tag{19}$$

is the variance of the interaction tensor projected along $\boldsymbol{q}$.

The ensemble average is taken by using the m-particle distribution functions $\rho^{(m)}(\boldsymbol{R}_1,\ldots,\boldsymbol{R}_m)$ of the centres of the spheres. In our approximation, we require only the two- and three-particle distribution functions, and in terms of these functions f_e can be written as

$$f_e = f_e^{(2)} + f_e^{(3)}, \tag{20}$$

where

$$f_e^{(2)} = 3f \int_0^\infty \frac{\rho^{(2)}(2a_0 x)}{x^4}\, \mathrm{d}x, \tag{21}$$

and

$$f_e^{(3)} = \frac{9}{4\pi^2} f^2 \int \hat{\boldsymbol{q}} \cdot \overleftrightarrow{\boldsymbol{T}}_{12} \cdot \overleftrightarrow{\boldsymbol{T}}_{23} \cdot \hat{\boldsymbol{q}} \Delta\rho^{(3)}(\boldsymbol{R}_1, \boldsymbol{R}_2, \boldsymbol{R}_3) d^3R_2 d^3R_3. \tag{22}$$

Here $f_e^{(3)}$ is independent of $\boldsymbol{R}_1$ due to the homogeneity of the ensemble, and

$$\Delta\rho^{(3)} \equiv \rho^{(3)}(\mathbf{R}_1, \mathbf{R}_2, \mathbf{R}_3) - \rho^{(2)}(\mathbf{R}_1, \mathbf{R}_2)\rho^{(2)}(\mathbf{R}_2, \mathbf{R}_3). \tag{23}$$

The solution of Eq. (17) is

$$\frac{\tilde{\alpha}^*}{2} = \frac{1 - \sqrt{1 - f_e\tilde{\alpha}^2}}{f_e\tilde{\alpha}}, \tag{24}$$

which has the *additional* broadening, mentioned above, induced by the effects of disorder. This can be easily seen by taking in Eq. (24) a polarizability $\tilde{\alpha}$ with a single isolated pole of zero width in $Im\tilde{\alpha}$. In this case $\tilde{\alpha}^*$ will acquire an imaginary part in the frequency region whenever $f_e\alpha^2 < 1$.

Substituting now Eq. (24) into Eq. (16) one finally gets,

$$\frac{\epsilon_M - \epsilon_b}{\epsilon_M + 2\epsilon_b} = 2f \left[\frac{1 - \sqrt{1 - f_e\tilde{\alpha}^2}}{f_e\tilde{\alpha}} \right]. \tag{25}$$

It is interesting to notice that in the case of low polarizability and/or small filling fraction, or more precisely, when $f_e\,|\,\tilde{\alpha}^2\,| \gg 1$, one can expand the square root in Eq. (25), in a power series in $f_e\tilde{\alpha}^2$, that is,

$$\frac{\epsilon_M - \epsilon_b}{\epsilon_M + 2\epsilon_b} = f\tilde{\alpha}\left[1 + \frac{1}{4} f_e\tilde{\alpha}^2 + \ldots\right]. \tag{26}$$

This yields to lowest order in $f_e\tilde{\alpha}^2$, the correction to the Clausius–Mossotti relation proposed by Kirkwood and Yvon (KY) [17], about fifty years ago, in their statistical theory of the dielectric response of non-polar liquids and dense gases.

In Ref. [11], ϵ_M was calculated taking $f_e^{(3)} = 0$, which is valid only in the low-density regime. At higher densities the effects of the three-particle correlations in ϵ_M should be important. Our purpose here is to analyze these effects using the best-known results for f_e.

Since the quantity f_e appears already in the theory of Kirkwood and Yvon, there have been many efforts to calculate it for a system of molecules in thermodynamic equilibrium. The main difficulty has been the lack of a precise knowledge of $\rho^{(2)}$ and $\rho^{(3)}$. There are different approximations for $\rho^{(2)}$ coming from the solution of the Ornstein–Zernike equations [18] for different kinds of intermolecular potentials. For a homogeneous system of hard spheres in thermodynamic equilibrium a useful approximation for $\rho^{(2)}$ is the one proposed by Percus and Yevick [19] in 1958. The calculation of $\rho^{(3)}$ is obviously a lot more difficult and a common simplifying approximation is the so called *superposition* approximation (SA), given by

$$\rho_{SA}^{(3)}(\mathbf{R}_1, \mathbf{R}_2, \mathbf{R}_3) = \rho^{(2)}(\mathbf{R}_{12})\rho^{(2)}(\mathbf{R}_{23})\rho^{(2)}(\mathbf{R}_{13}), \tag{27}$$

valid at low densities. A more precise determination of both $\rho^{(2)}$ and $\rho^{(3)}$ has been possible through numerical simulation techniques. For example, for a system of hard spheres a reliable Monte–Carlo simulation for $\rho^{(2)}$ has been available [20] since 1972. Nevertheless, there is no need to know $\rho^{(2)}$ and $\rho^{(3)}$ explicitly for the calculation of the integrals in f_e, because the ensemble averaged themselves given in Eq. (19), can be also numerically simulated.

In Fig. 1 we show the results for f_e, properly scaled, collected by Stell and Rushbrooke [21] for different approximations for $\rho^{(2)}$ and $\rho^{(3)}$ as well as for a

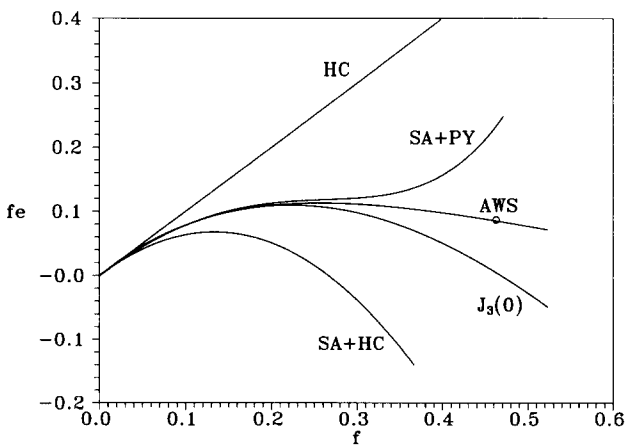

Fig. 1. f_e as a function of f, as defined by Eq. (18). The point labelled AWS corresponds to the numerical simulation done by Alder, Weis and Strauss [23]. The other symbols are defined in the text.

numerical simulation using a Monte–Carlo technique. Here HC is the simplest approximation, it means $f_e^{(3)} = 0$ and $\rho^{(2)} = \rho_{HC}^{(2)} \equiv \theta(R_{12} - 2a_0)$. HC stands for *hole correction*; it accounts only for the correlations coming from the excluded volume of the spheres. SA + HC means that $\rho^{(3)}$ was taken using the SA and $\rho^{(2)} = \rho_{HC}^{(2)}$. In $J_3(0)$, $f_e^{(2)}$ was calculated numerically using a Monte–Carlo technique [22] and for $f_e^{(3)}$ the integral was performed using SA for $\rho^{(3)}$ with $\rho^{(2)} = \rho_{HC}^{(2)}$. SA + PY means that $\rho^{(3)}$ was taken using the SA and $\rho^{(2)}$ within the Percus–Yevick approximation. Finally, the point labelled AWS corresponds to a numerical simulation done by Alder et al. [23] using a Monte–Carlo technique. This calculation was done for a single filling fraction $f = 0.4628$ and the rest of the curve is an extrapolation of what Stell and Rushbrooke believe is the best available prediction; here we will call this curve $f_e(AWS)$. As it can be seen, at low filling fractions ($f \leqslant 0.05$) all curves coincide with $f_e = f$. It is obvious too that both, the contribution of $f_e^{(3)}$ and a more accurate estimation of $f_e^{(2)}$, become extremely important the higher the filling fraction. Taking the curve $f_e(AWS)$ as our best choice, it can be seen that the use of the SA in f_e starts to break down at $f \cong 0.3$ and for $f \cong 0.45$ it is off by a factor of two. Furthermore, comparing $f_e = f$ with AWS for $f \cong 0.45$, the difference is at least a factor of five. Notice also that $f_e = 0$ corresponds, in RPT, to the MFA.

In the case of a composite made of a solid homogeneous matrix with spherical inclusions, the calculation of $\rho^{(2)}$ and $\rho^{(3)}$ should take into account the specific process through which the composite was made, and it would not necessarily correspond to a system of hard spheres in thermodynamic equilibrium. Nevertheless since an accurate determination of $\rho^{(2)}$ and $\rho^{(3)}$ for any specific composite would be almost impossible, here we will take the value of f_e given by $f_e(AWS)$ as a guidance for analysing the effects of two- and three-particle correlations in the effective dielectric response. Furthermore, a comparison between theory and experiment has been a difficult task because the samples used in the laboratory are far from being a collection of identical spheres. Usually there is a distribution of sizes and shapes in the inclusions as well as clustering effects. On the other hand, experimentalists were used to report only the filling fraction of their samples forgetting about other relevant properties of the microstructure, like the two-particle distribution function. Thus, even the comparison between different experimental results might not be legitimate, because one could have samples with the same filling fraction but with different microstructures. Under these circumstances, the only fair comparison nowadays between theory and experiment is the comparison between theory, and *numerical experiments* which solve the same model under the same approximations. Fortunately the results of these numerical simulations are now available [12,24].

3. Results

Here we calculate ϵ_M by substituting in Eq. (25) the value of f_e given by $f_e(AWS)$ and compare them with the results of Ref. [11], where $f_e^{(3)} = 0$, and with numerical simulations done on the same model.

We perform this analysis through the Bergman representation [25] of the spectral function $g(u)$, defined through the relation

$$\frac{\epsilon_M}{\epsilon_b} = 1 - \int_0^1 \frac{g(u)}{t-u}\,\mathrm{d}u, \tag{28}$$

where

$$t = \frac{1}{1-\epsilon_s/\epsilon_b}. \tag{29}$$

The spectral function gives the weights of the different optically-active electromagnetic modes of the system. Its main advantage is that it does *not* depend on the dielectric properties of the materials but only on the geometry and the spatial distribution of the inclusions. It also obeys the following sum rules:

$$\int_0^1 g(u)\,\mathrm{d}u = 1, \quad \int_0^1 ug(u)\,\mathrm{d}u = \tfrac{1}{3}(1-f). \tag{30}$$

The spectral function was obtained by solving Eq. (28) for $g(u)$, that is,

$$g(u) = \frac{1}{\pi f}\mathrm{Im}\left[\lim_{s\to 0}\epsilon_M(u+is)/\epsilon_b\right]. \tag{31}$$

In the MFA, $g(u)$ turns out to be

$$g(u) = \delta[u-(1-f)/3], \tag{32}$$

where δ is the Dirac delta function. This simply means that in this approximation there is only one optically-active mode.

On the other hand, in the RPT $g(u)$ becomes

$$g(u) = \frac{1}{\pi}\frac{6\sqrt{f_e-(1-3u)^2}}{4f^2-4f(1-3u)+f_e}\theta(u-u_L)\theta(u_U-u) + \left(f-\frac{f_e}{4f}\right)\theta(4f^2-f_e)\delta(u-u_S), \tag{33}$$

where

$$u_L = \tfrac{1}{3}\left(1-\sqrt{f_e}\right),\ u_U = \tfrac{1}{3}\left(1+\sqrt{f_e}\right), \text{ and } u_S = \frac{1-f}{3} - \frac{f_e}{12f}. \tag{34}$$

It can be seen, that $g(u)$ is no longer a single pole as in the case of the MFA, it has now structure for all $u_L \leqslant u \leqslant u_U$ plus an isolated pole at $u = u_S$ for $f \geqslant \sqrt{f_e}/2$. It can also be checked that it fulfils the sum rules given in Eq. (30).

In Fig. 2 we show different calculations of $g(u)$ for $f = 0.3$. The dashed line corresponds to RPT with $f_e^{(3)} = 0$ and $f_e^{(2)}$ calculated with $\rho_{HC}^{(2)}$, the solid line to RPT with $f_e(AWS)$ and the dotted line to the numerical simulations done by Felderhof and Cichocki [12] for the same model with the same approximations. In comparing the dashed with the solid curve, we can see that the main effect of

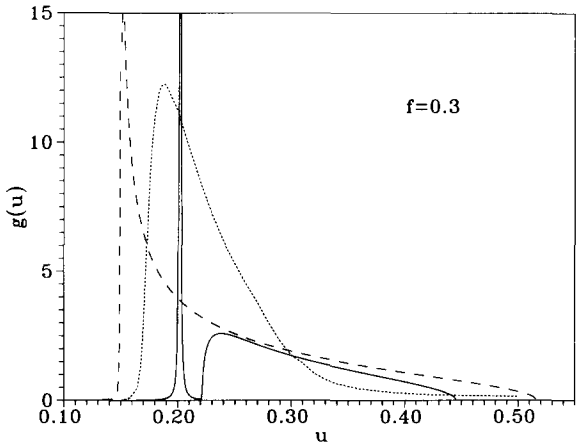

Fig. 2. The spectral function $g(u)$ as a function of u for a filling fraction $f = 0.3$. The broken line corresponds to RPT with $f_e^{(3)} = 0$ and $\rho_{HC}^{(2)}$. The solid line corresponds to RPT with f_ϵ(AWS). The dotted line is the computer simulation of Ref. [12].

taking more accurate values of $\rho^{(2)}$ and $\rho^{(3)}$ is to shift the peak of $g(u)$ to higher values of u, giving a better agreement between the solid curve and the one corresponding to the numerical simulation. In the solid curve there is an isolated pole, which has no physical significance and should be a consequence of the approximations used in RPT. Nevertheless this isolated pole broadens and merges with the rest of the structure when the effects of nonradiating damping are taken into account yielding a single broad peak. This is shown in Fig. 3 where we plot three different curves for $Im\epsilon_M(\omega)$ as a function of ω/ω_p, for a system of spheres

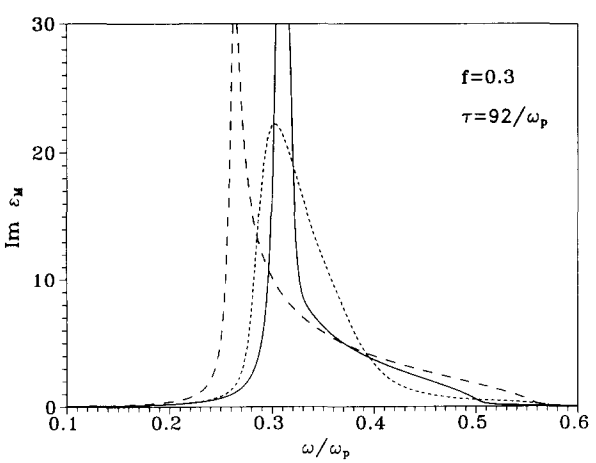

Fig. 3. Im ϵ_M as a function of ω/ω_p for Drude spheres in gelatin ($\epsilon_b = 2.37$) and a filling fraction $f = 0.3$. Here $\tau = 92/\omega_p$. The three curves, solid, dashed and dotted, were obtained through Eq. (28) using the corresponding solid, dashed and dotted curves for $g(u)$ given in Fig. 2.

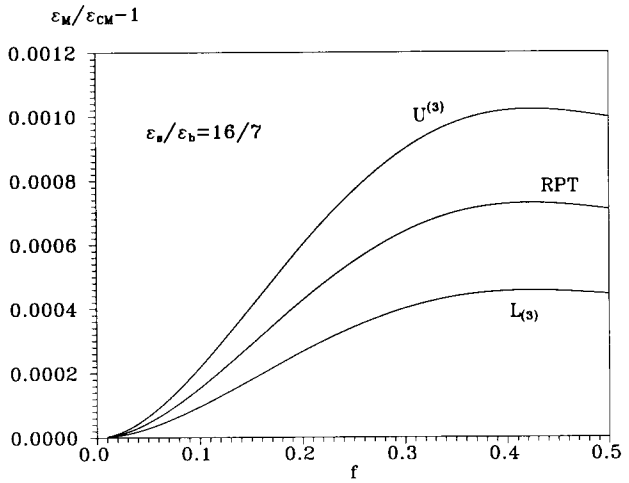

Fig. 4. The relative deviation $\epsilon_M/\epsilon_{CM}-1$, from the Clausius–Mossotti value ϵ_{CM}, calculated with RPT for a system with $\epsilon_s/\epsilon_b = 16/7$. Curve $U^{(3)}$ ($L(3)$) corresponds to the dipolar contribution to the third order upper (lower) bound of Ref. [26].

with a Drude dielectric function and a finite electronic relaxation time $\tau = 92/\omega_p$, embedded in dispersionless gelatin ($\epsilon_b = 2.37$). The three curves, solid, dashed and dotted, were obtained through Eq. (28) using the corresponding $g(u)$ given in Fig. 2. One can see, that although the shape is not exactly the same, the position of the absorption peak of the solid curve coincides with the one of the numerical simulation (dotted).

Now we show the results of RPT for ϵ_M, in the frequency region far from the resonances, where the materials are transparent and dispersionless, that is, when ϵ_s and ϵ_b are real and independent of ω. In this case the polarizability of the spheres $\tilde{\alpha} = [\epsilon_s - \epsilon_b]/[\epsilon_s + 2\epsilon_b]$ is also real and ϵ_M can be computed directly from Eq. (25).

In Fig. 4 we illustrate the behavior of the deviations of ϵ_M calculated with RPT with respect to the Clausius–Mossotti value ϵ_{CM}. We plot $\epsilon_M/\epsilon_{CM}-1$ as a function of f, for a system with contrast $\epsilon_s/\epsilon_b = 16/7$. The dipolar contribution to the third-order bounds derived by Felderhof [26] is also included in this figure. These bounds are third-order because they involve up to a three-particle distribution function. The upper bound $U^{(3)}$ and the lower bound $L_{(3)}$ are given by

$$U^{(3)} = \epsilon_s\left(1 - \frac{h_1}{1-t} - \frac{h_2}{(1-t)(1-t-h_3/h_2)}\right), \tag{35}$$

and

$$L(3) = \epsilon_b\left(1 - \frac{e_1}{1-t} - \frac{e_2}{(1-t)(1-t-e_3/e_2)}\right)^{-1}, \tag{36}$$

where

$$e_1 = f, \qquad e_2 = \frac{2f}{3}(1-f), \qquad e_3 = \frac{4f}{9}(1-f)^2 + \frac{f}{36}f_e,$$

$$h_1 = 1-f, \qquad h_2 = \frac{f}{3}(1-f), \qquad h_3 = \frac{f}{9}(1-f)(2+f) - \frac{f}{36}f_e, \qquad (37)$$

the parameter t is given by Eq. (29) and $\epsilon_s > \epsilon_b > 0$. The parameter f_e is common to RPT as well as to $U^{(3)}$ and $L_{(3)}$. In Fig. 4 all the curves have been calculated using $f_e(AWS)$. One can see that the RPT curve lies well within the bounds and it is interesting to point out that these calculations are very sensitive to the value of f_e.

4. Conclusions

We have presented a simple theory, within the quasistatic, dipolar approximation, for the calculation of the effective dielectric response of a system of spherical inclusions located at random positions and embedded in an otherwise homogeneous matrix. The theory goes beyond the MFA and takes account of the dipolar fluctuations through a single scalar parameter α^* which can be interpreted as a renormalized polarizability. The value of α^* is determined by solving an algebraic second order equation with coefficients that involve the bare polarizability α and a parameter f_e, which depends on the filling fraction f and integrals involving the dipole–dipole interaction and the two- and three-particle distribution functions. The parameter f_e has been calculated previously [21] using different approximations for both the two-and three-particle distribution functions. The most reliable values of f_e are the ones obtained using an extrapolation which passes through a value calculated by a Monte–Carlo simulation for $f = 0.4628$. These values were used to calculate α^* and then the effective dielectric response ϵ_M and the spectral function $g(u)$. The results were compared with a previous version of the theory which used a crude approximation of f_e, Ref. [11], and also with the results of a numerical simulation. We found that the effect of the dipolar fluctuations is to produce, in $g(u)$, an asymmetric peak with a finite width, in contrast with the single delta function in the MFA. Also, a more accurate value of f_e in α^* blue-shifts the absorption peak of $Im\epsilon_M$ with respect to the results reported in Ref. [11], yielding a better agreement with the numerical simulation. This was shown for a system of silver particles embedded in gelatin and $f = 0.3$. On the other hand, for transparent materials the values of ϵ_M calculated through α^* fall inside the third-order bounds.

Although α^* contains an additional broadening of the absorption peaks induced by disorder, the comparison of the profile of $g(u)$ with the results of numerical simulations is still not good enough, even when the best available values of f_e are used. A better agreement would require a more accurate and obviously a more involved treatment of the dipolar fluctuations.

Acknowledgements

The authors acknowledge fruitful discussions with W. Luis Mochán, Cecilia Noguez, Francisco Claro and Ronald Fuchs. This work was partially supported by Dirección General de Asuntos del Personal Académico and Coordinación General de Estudios de Posgrado of the Universidad Nacional Autónoma de México under grants IN-102593 and PADEP-003004, respectively.

References

[1] J.C. Maxwell, Treatise on Electricity and Magnetism, Vol. 1 (Oxford, Clarendon Press, 1873) p. 360.
[2] J.W.S. Rayleigh, Philos. Mag. 34 (1892) 481.
[3] J.C. Maxwell Garnett, Philos. Trans. R. Soc. London 203 (1904) 385.
[4] R. Landauer, Transport and optical properties of inhomogeneous media (ETOPIM1), in: J.C. Garland and D.B. Tanner (Eds.), Electrical AIP Conference Proceedings No. 40 (AIP, New York, 1978) p. 2.
[5] N.E. Cusack, The Physics of Structurally Disordered Matter (Hilger, Bristol, 1987).
[6] See for example: G.A. Niklasson and C.G. Granqvist, in: J. Davenas and P.M. Rabette (Eds.), Contribution of Cluster Physics to Materials Science and Technology, Vol. 104 of NATO Advanced Study Institute (Nijhoff, Dordrecht, 1986) p. 539.
[7] O.F. Mossotti, Mem. di Matem. e Fisica della Soc. Ital. della Sci. Residente in Modena 24, 49 (1850). R. Clausius, Die Mekanische Warmetheorie, 2nd Ed., Vol. 2, Section 3 (Braunschweig, Vieweg, 1879) p. 62.
[8] R.G. Barrera, M. del Castillo-Mussot, G. Monsivais, P. Villaseñor and W.L. Mochán, Phys. Rev. B 43 (1991) 13819; J. Vlieger and D. Bedeaux, Thin Solid Films 69 (1980) 107; D. Bedeaux and J. Vlieger, Thin Solid Films 102 (1983) 265.
[9] R.G. Barrera, J. Giraldo and W.L. Mochán, Phys. Rev. B 47 (1993) 8528.
[10] R.G. Barrera, G. Monsivais, W.L. Mochán and E. Anda, Phys. Rev. B 39 (1989) 9998; R.G. Barrera, C. Noguez and E. Anda, J. Chem. Phys. 96 (1992) 1574; B.U. Felderhof, J. Phys. C 15 (1982) 1731, 3943, 3953; Physica A 126 (1984) 430.
[11] R.G. Barrera, G. Monsivais and W.L. Mochán, Phys. Rev. B 38 (1988) 5371.
[12] B. Cichocki and B.U. Felderhof, J. Chem. Phys. 90 (1989) 4960.
[13] F. Claro and R. Rojas, Phys. Rev. B 43 (1991) 6369; L. Fu, P.B. Macedo and L. Resca, Phys. Rev B 47 (1993) 13818.
[14] R.C. McPhedran and D.R. McKenzie, Proc. R. Soc. London, Ser. A 359 (1978) 45; L. Poladian and R.C. Mc Phedran, Proc. R. Soc. London, Ser. A 408 (1986) 45.
[15] B.U. Felderhof, in R.G. Barrera and W.L. Mochán (Eds.), Physica A, Proceedings of the Third International Conference on Electrical Transport and Optical Properties of Inhomogeneous Media (ETOPIM3) (to be published).
[16] See for example: R.G. Barrera, G. Monsivais, W.L. Mochán and E. Anda, Phys. Rev. B 39 (1989) 9998; R.G. Barrera, C. Noguez and E. Anda, J. Chem. Phys. 96 (1992) 1574 and references therein.
[17] J.G. Kirkwood, J. Chem. Phys. 4 (1936) 592; J. Yvon, Recherches sur la Théorie Cinétique des Liquides (Hermann, Paris, 1937).
[18] L.S. Ornstein and F. Zernike, Proc. K. Ned. Akad. Wet. 17, (1914) 793.
[19] J.K. Percus and G.J. Yevick, Phys. Rev. 110 (1958) 1.
[20] L. Verlet and J.J. Weis, Phys. Rev. A 5 (1972) 939.
[21] G. Stell and G.S. Rushbrooke, Chem. Phys. Lett. 24 (1974) 531.
[22] G.S. Rushbrooke, G. Stell and J.S. Hoye, Mol. Phys. 26, (1973) 1199.

[23] B.J. Alder, J.J. Weis and H.L. Strauss, Phys. Rev. A 7 (1973) 281.
[24] S. Kumar and R.I. Cukier, J. Phys. Chem. 93 (1989) 4334.
[25] D.J. Bergman, Electrical transport and optical properties of inhomogeneous Media (ETOPIM1), in: J.C. Garland and D.B. Tanner (Eds.), AIP Conference Proceedings No. 40 (AIP, New York, 1978), p. 46; Phys. Rev C 43 (1978) 377; Ann. Phys. (N.Y.) 138 (1982) 78.
[26] B.U. Felderhof, J. Phys. C: Solid State Phys. 15 (1982) 3953.